Contents lists available at ScienceDirect

Colloids and Surfaces A: Physicochemical and Engineering Aspects

journal homepage: www.elsevier.com

Efficiency of granulocyte colony-stimulating factor immobilized on magnetic microparticles on proliferation of NFS-60 cells

Anton Popov [a, b], Arunas Stirke [c], Neringa Bakute [c], Benediktas Brasiunas [a], Arunas Ramanavicius [a, d], Almira Ramanaviciene [a, b, *]

[a] NanoTechnas – Center of Nanotechnology and Material Science, Faculty of Chemistry and Geosciences, Vilnius University, Naugarduko st. 24, LT-03225, Vilnius, Lithuania
[b] Department of Immunology, State Research Institute Centre for Innovative Medicine, Santariskiu str. 5, LT- 08406, Vilnius, Lithuania
[c] Laboratory of Bioelectrochemistry, State Research Institute Center for Physical Sciences and Technology, Sauletekio ave. 3, LT-10257, Vilnius, Lithuania
[d] Department of Physical Chemistry, Faculty of Chemistry and Geosciences, Vilnius University, Naugarduko 24, LT-03225, Vilnius, Lithuania

ARTICLE INFO

Keywords:
Granulocyte colony-stimulating factor
Magnetic particles
Biomodification
Cell proliferation

ABSTRACT

Magnetic particles are promising carriers for targeted drug delivery. Granulocyte colony-stimulating factor (G-CSF) is a cytokine which stimulates neutrophil proliferation process. In this study, G-CSF molecules were successfully covalently immobilized on magnetic silica gel beads (MagBs) surface. Comparison of free and on MagBs immobilised G-CSF (MagBs-G) on proliferation efficiency and viability of mouse myeloid cell line NFS-60 was performed using XTT assay. Cytotoxic or stimulation effects of used MagBs on NFS-60 cell proliferation were not observed. However, the positive effect on proliferation of cells was noticed increasing the concentration of MagB-G in the test wells from 0.5 μg/ml to 50 μg/ml. Proliferation of cells in the presence of 50 μg/ml MagBs-G (2.7 μg/ml G-CSF) resulted in maximal proliferation response, which was reached using free G-CSF. Comparing the concentration of G-CSF that gives half-maximal response of free (3.6 pM) and on MagBs immobilized (11.4 nM) G-CSF can be concluded that immobilized G-CSF possessed the same efficiency as free G-CSF molecules, however the higher amount of immobilized G-CSF is required.

1. Introduction

Nowadays magnetic micro- and nanoparticles (MPs) are used in a wide variety of applications particularly for *in vitro* biomedical diagnostic and bionanotechnology [1]. MPs consist of magnetic elements (mostly of iron, nickel, cobalt and their chemical compounds) and can be manipulated using external magnetic field. This property of MPs simplifies their modification procedure [2,3]. Iron oxide particles such as magnetite (Fe_3O_4) or its oxidized form maghemite (γ-Fe_2O_3) are mostly used magnetic core in biomedical applications due to their good biocompatibility and biodegradability [4]. Moreover, MPs of different size (from a few nanometers to micrometers) made of iron oxide are commercially available and can be modified or encapsulated in polymers, metals, silica or carbon materials [5,6]. The magnetic properties of modified MPs depend on the size of the core. Usage of multiple small cores encapsulated by a single shell allows to improve MPs properties [7]. The coating of MPs can change their surface area and charge, however functional groups present on the surface of coatings ensure better immobilization of ligand for molecular targeting. Most often proteins on the surface of MPs are immobilized by physical adsorption or covalent bonding. Adsorption is a simple, quick and inexpensive immobilization method which is characterized by a random orientation of proteins and weak attachment on the surface. Covalent bonding or cross-linking provides stronger attachment of proteins on the surface, however more than one reactive group is usually required for protein immobilization and stable ligand layer formation [8–10].

Fabricated magnetic particles-based approaches have been proposed for various biomedical applications. Based on the functions, MPs can be used for gene and drug delivery [11], DNA separation [12], biosensing [13] (for instance, protein detection by magnetorotation [14], protein barcoding [15]) and in magnetic resonance and magnetic particles imaging [16,17]. Moreover, interaction between MPs and target cells may induce various side-effects and might have a negative impact to viability and cell functions [18–20]. Generation of reactive oxygen species during biodegradation and leaching of MPs has the highest impact on cell viability [21].

* Corresponding author at: NanoTechnas – Center of Nanotechnology and Material Science, Faculty of Chemistry and Geosciences, Vilnius University, Naugarduko st. 24, LT-03225, Vilnius, Lithuania.
Email address: almira.ramanaviciene@chf.vu.lt (A. Ramanaviciene)

https://doi.org/10.1016/j.colsurfa.2019.123580
Received 22 February 2019; Received in revised form 17 June 2019; Accepted 17 June 2019
Available online xxx
0927-7757/

Granulocyte colony-stimulating factor (G-CSF) is an important biological drug, which is in the first ten positions of biopharmaceutical sales [22,23]. This protein acts on the neutrophil lineage selectively stimulating the proliferation and differentiation of committed progenitor cells and activation of mature neutrophils [24,25]. G-CSF action is modulated though binding to the granulocyte colony-stimulating factor receptor by forming a homo-oligomeric complex. G-CSF also exerts a direct effect on retinal photoreceptor cells [26], glioma cells [27], myoblast [28] and other types of cells.

In the present study, we explored and compared the effect of free and on magnetic silica gel beads (MagBs) immobilized G-CSF on the proliferation of cells. A mouse myeloid cell line (NFS-60) has been chosen as a model system for this research. The distribution of MagBs in the cell culture, their cytotoxic or stimulating effect and influence of free and on MagBs immobilised G-CSF on the cell proliferation have been evaluated and compared. In addition, the efficiency of covalent G-CSF immobilization on MagBs has been determined, and the simplicity and convenience of MagBs for such purpose have been demonstrated.

2. Materials and methods

2.1. Materials

Phosphate buffered saline (PBS) tablets (0.0027 M KCl, 0.137 M NaCl, and 0.01 M phosphate buffer pH 7.4), 1-ethyl-3-(3-diaminopropyl) carbodiimide hydrochloride (EDC) were purchased from Sigma Aldrich (Germany). Tris(hydroxymethyl)-aminomethane (Tris), bovine serum albumin (BSA), magnetic silica gel beads Roti®-MagBeads COOH HP58 (10 ± 0.5 mg/ml) (MagBs), Bradford Reagent (5 times concentrated solution, Roti®-Nanoquant) and 4-Morpholineethanesulfonic acid monohydrate (MES) were obtained from Carl Roth (Germany). N-Hydroxysuccinimide (NHS) was received from Merck (Germany). Granulocyte-colony stimulating factor (G-CSF) was donated from Profarma UAB (Lithuania). Deionized (DI) water was obtained from a water purification system Adrona SIA (Latvia). Mouse myeloid cell line (NFS-60) received from Profarma UAB were grown in RPMI 1640 growth medium, fetal bovine serum, gentamicin sulphate, 2-mercaptoethanol [29]. 0.1 M PBS pH 7.4, 0.1 M Tris buffer, deionized water was autoclaved before using. All other solutions were prepared in the laminar Flow Hood (NuAire, USA) from autoclaved DI water and were passed through the 0.22 μm PES filter.

2.2. MagBs characterization

The size and morphology of MagBs were evaluated using high-resolution field emission scanning electron microscope (SEM) SU-70 (Hitachi, Japan) and transmission electron microscope (TEM) Tecnai G2 F20 X-TWIN (FEI, Netherlands). Absorbance spectra of MagBs was collected using double-beam spectrophotometer Lambda 25, PerkinElmer (Shelton, USA).

2.3. Immobilization of G-CSF on the MagBs

G-CSF molecules were attached by covalent coupling of amino groups to activated carboxyl groups on MagBs surface using carbodiimide crosslinkers chemistry. All immobilization procedures were performed in the laminar flow hood at room temperature. Before the immobilization, MagBs solution was resuspended by sonicating for 10 min. 10 μl of MagBs (10 ± 0.5 mg/ml) was added to 1 ml of 0.1 M MES buffer pH 5, gently mixed and supernatant was discarded by using magnetic separation. Washing procedure was carried out two times. To activate carboxyl groups on the surface of MagBs, freshly prepared 0.417 mM EDC and 0.695 M NHS solutions were mixed in the ratio 1:1 and poured on magnetic particles. Activation solution was mixed on a shaker for 20 min. Magnetic particles were collected by a magnet, washed once with 1 ml of 0.1 M MES buffer and supernatant was discarded. After that 200 μl of 0.05 mg/ml G-CSF solution prepared in 0.01 M PBS pH 7.4 was added to the activated MagBs. Suspension was mixed on a shaker for 2 h. Afterwards, MagBs modified with G-CSF molecules were collected with a magnet and supernatant was separated for the determination of residuary G-CSF concentration by Bradford protein assay. Meanwhile, particles were washed 3 times with 1 ml 0.01 M PBS pH 7.4. Uncoupled activated carboxyl groups on the surface of MagBs were blocked by keeping modified particles in 1 ml 0.1 M Tris buffer for 2 h while mixing on a shaker. In the end of the modification MagBs were washed 3 times with 1 ml 0.01 M PBS and 3 times with 1 ml 0.01 M PBS containing 1 mg/ml BSA. Magnetic particles with immobilized G-CSF (MagBs-G) were re-suspended in 200 μl 0.01 M PBS containing 1 mg/ml BSA and have been kept at + 4 °C.

2.4. Bradford assay

Calibration curves were built using BSA and G-CSF as standards in the range from 1 to 75 μg/ml and from 1 to 25 μg/ml, respectively. Disposable plastic cuvettes were filed with 200 μl each of standards (or sample) of corresponding concentrations and 800 μl Roti®-Nanoquant working solution. Each sample was measured at wavelengths of 590 nm and 450 nm. Ratio of absorbance at $A_{590\ nm}$ to $A_{450\ nm}$ was used for determination of protein concentration.

Residual supernatant after G-CSF immobilization on the MagBs step was analysed in the Roti®-Nanoquant assay range, diluting each sample 4 times to fit the $A_{590\ nm}/A_{450\ nm}$ ratio in the linear zone of the calibration curve.

2.5. Cell culture and treatment

Biological activity of G-CSF proteins was determined using NFS-60 cell line [30]. Active G-CSF protein initiates proliferation of this cell line after interaction with G-CSF receptor on the surface of the cells [31]. NFS-60 cells were maintained in RPMI 1640 growth medium supplemented with 10% fetal bovine serum, antibiotic – gentamicin sulphate, 0.05 mM 2-mercaptoethanol and 2 ng/ml G-CSF monomer. Before determination of biological activity of G-CSF monomer, NFS-60 cells were prepared: centrifuged and re-suspended at a concentration of 5.0×10^7 cells/ml in cell maintenance media without G-CSF and 2-mercaptoethanol.

For the test procedure, G-CSF was serially diluted in growth medium for the investigation of NFS-60 cell proliferation in the presence of free G-CSF. MagBs and MagBs-G were serially diluted in 0.01 M PBS pH 7.4 containing 1 mg/ml BSA. 40 μl of growth medium RPMI 1640 supplemented with 10% fetal bovine serum and 10 μl of solution containing required concentration of free G-CSF, MagBs or MagBs-G were aliquoted per test well of 96-well tissue culture plate. The final concentrations of free G-CSF were from 0.01 μg/ml to 1 μg/ml, MagBs – from 0.5 μg/ml to 100 μg/ml and MagBs-G – from 0.5 μg/ml to 50 μg/ml, respectively. Each concentration of free G-CSF, MagBs or MagBs-G was tested in triplicate. Effect of MagBs on cells proliferation was studied in presence of 2 ng/ml free G-CSF in grown medium. 2-mercaptoethanol was added to the prepared cell suspension to a final concentration of 0.1 mM and 50 μl of such NFS-60 cells was added into each test well (1×10^4 cells/well). The plates were incubated for 48 h at 37 °C in a 5% CO_2 atmosphere.

2.6. Cell proliferation and viability assay

XTT is a colorimetric assay used to assess cell viability as a function of cell number based on metabolic activity [32]. After 48 h of NFS-60 cell incubation with free G-CSF, MagBs or MagBs-G, test wells were

filled with XTT reagent and incubated for another 6 h maintaining the 37 °C temperature and 5% CO_2. The absorbance of converted dye which is linked to the viable cells was measured at 490 nm using a microplate reader.

3. Results and discussion

Various nanoparticles are increasingly employed in medicine for diagnosis, therapy or drug delivery. In recent years increasing attention has been given to the development of new strategies of therapeutic agent's delivery to the target and for increase circulation time *in vivo* of these agents. Application of magnetic micro- and nanoparticles as a core for a drug carrier ensure localized drugs transport by applying a magnetic field over the target, while immobilisation of drugs on the carrier provides longer circulation time keeping drugs activity [33,34]. Additionally, it was observed that some carriers (diethylenetriaminepentaacetic acid functionalized SiO_2 nanoparticle) have stimulating effect on the cell proliferation without any modification with drugs [35]. Biocompatibility and magnetic properties of particles can be improved by encapsulating MPs in a shell [36,37]. In this study used MagBs consisted of Fe_3O_4 nanoparticles coated by silica matrix, which protects cells from the cytotoxic effect of magnetite or its oxidized form maghemite.

The characterization of MagBs was performed before immobilization of G-CSF by different techniques (Fig. 1). It was determined from SEM and TEM images that particles were spherical. The presence of Fe_3O_4 nanoparticles in silica matrix can be observed in TEM image (Fig. 1B). The size distribution was evaluated from SEM images. The average size of MagBs was 571 ± 171 nm (Fig. 1C). Although the particles were not exactly the same size, MagBs were well suited for immobilization of G-CSF. MagBs were easily collected during all stages of MagBs-G preparation. In addition, possible influence of MagBs presence in solution on XTT results was evaluated by recording MagBs absorbance spectra (Fig. 1D). The absorbance of MagBs solution gradually decreases in range from 350 to 800 nm, wherein absorbance of 100 µg/ml MagBs solution at 490 nm was equal to 0.067. Considering, that such MagBs concentration was the highest concentration, which was used in following experiments, it can be concluded that presence of MagBs in solution should not influence XTT results.

The cytotoxic or stimulating effect of MagBs used in our study on cells was evaluated by XTT colorimetric assay after culturing of NFS-60 cells in the presence of 2 ng/ml free G-CSF and varying concentrations of MagBs (from 0.5 to 100 µg/ml) in a 96- well microplate for 48 h (Fig. 2). Cell viability expressed in percentage and normalized to the control (100% without MagBs) was higher than 88% in all cases. Moreover, no dependencies between viability of cells and MagBs concentration were determined. Thus, MagBs used in our study are neither cytotoxic, nor exhibited a stimulating effect on the cells. Fig. 3 represents differences between how cells look like immediately after the addition of MagBs to the culture medium and after 48 h of cultivation. Shortly after the addition of MagBs (Fig. 3A) most of magnetic particles were located away from cells. Besides, the majority of MagBs were isolated from each other, although portion of particles were interconnected in chains or formed structures of pellet shape. After 48 h of incubation (Fig. 3B) the number of cells increased. Almost all magnetic particles were clustered in chains or structures of pellet shape. Furthermore, most of interconnected MagBs were located close to the cells. Only a small part of MagBs was located separately from each other. In conclusion, MagBs are prone to interconnection and migration towards cells after 48 h of cultivation. Similar tendency was observed in subsequent experiments with MagBs modified with G-CSF.

In XTT assay the change of solution colour from slightly yellow to bright orange is proportional to the number of viable cells [38]. In the case of high colorimetric reaction intensity, yellow colour turns to red.

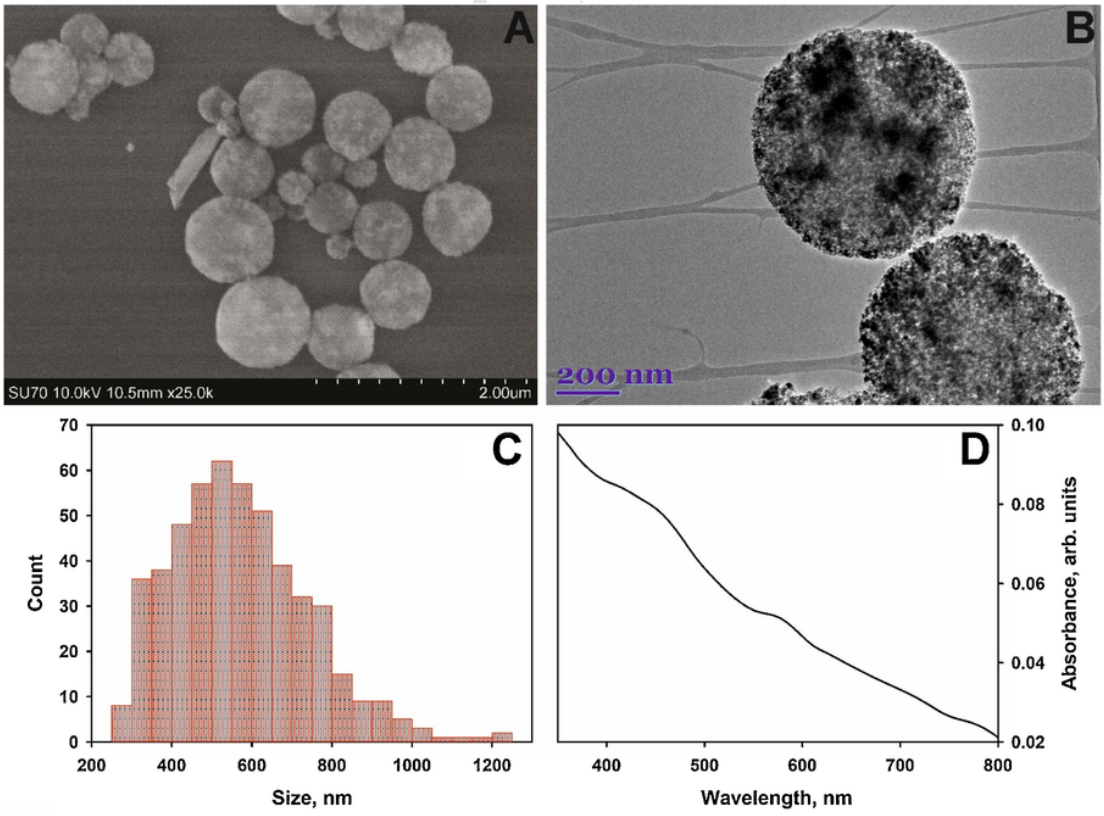

Fig. 1. Characterization of magnetic silica gel beads by different methods. (**A**) SEM and (**B**) TEM images of MagBs. (**C**) The size distribution of MagBs obtained from SEM images. (**D**) Absorbance spectra of MagBs solution (C_{MagBs} = 100 µg/ml).

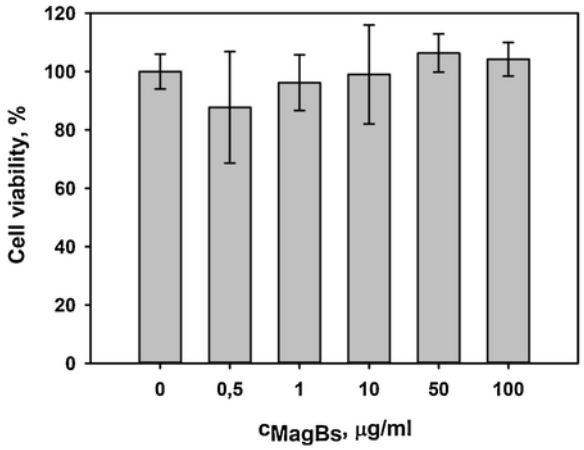

Fig. 2. Dependence of cell viability on the concentration of magnetic silica gel beads determined by XTT assay.

Magnetic silica gel beads, which were used in our investigation, were of brown colour (Fig. 3). Therefore, it was decided to additionally investigate how the colour of MagBs could influence the results of an XTT assay. In order to accomplish this task two experiments were performed in parallel (Fig. 4). The first one was performed in the same way as the investigation of the cytotoxic or stimulating effect of MagBs on cells. NFS-60 cells were incubated in the presence of various MagBs concentrations. Cell viability was evaluated by XTT colorimetric assay. The second one was done in the same way as the first, except that MagBs were removed from the medium with cells before analysis. The solution of growing cells with MagBs was poured into 1.5 ml tube after 48 h of cultivation. MagBs were collected with a magnet on the side of tubes. Supernatant without MagBs was used for XTT colorimetric analysis. The absence of MagBs in the growing medium with cells was confirmed by optical microscopy. The effect of MagBs presence in the test well and their colour on the results of cell viability determined by XTT assay is shown in Fig. 4.

Based on XTT assay results, the decrease or increase of cell viability for analysis using growth medium with cells and MagBs was not greater than 10%. These results are comparable with previously presented data (Fig. 2). XTT cell proliferation assay showed that removal of MagBs by a magnet from the growth medium with cells had a negative influence on the test results in all samples with a different concentration of MagBs. This negative effect changed very little with the increase of MagBs concentration in the growth medium with cells. A lower viability of cells associated with lower absorbance of converted dye in solutions without MagBs in comparison with the control can be explained by a loss of cells during MagBs removing procedure. After 48 h of incubation most of magnetic particles were located close to cells (Fig. 3B), therefore magnetically discarding MagBs might mutually results in a removal of cells. Furthermore, during the MagBs removal from the medium with cells, an additional procedure of pouring the solution into tubes and back to the plate wells was performed and therefore the additional loss of some cells can occur. Finally, considering that previously determined absorption of the 100 µg/ml concentration of MagBs at 490 nm is 0.067 it can be concluded that MagBs presence when performing XTT assay is negligible.

The success of MagBs modification with G-CSF was evaluated by analysing supernatant that was obtained after the removal of modified MagBs-G. Bradford assay was used for the determination of residual G-CSF in a 4 times diluted supernatant. Different additives, salts and the dilution of a sample in buffers have extensive effects on the protein calibration curve obtained by the Bradford assay [39,40]. Two calibration curves of BSA were prepared. Deionized water or 0.01 M PBS, pH 7.4, were used for the dilution of BSA stock solution and the preparation of calibration curves. It was observed that the slope of the calibration curve was 15% higher using water compared to PBS. The presence of hydrogen phosphate and dihydrogen phosphate ions (HPO_4^{2-} and H_2PO_4-) in the solution can increase aggregation of the proteins [41]. So, considering that for the modification procedure the stock solution of G-CSF was diluted with PBS it was decided to use 0.01 M PBS, pH 7.4, for the preparation of BSA calibration curve. Additionally, a calibration curve of G-CSF employing PBS to dilute stock solution was prepared. The difference of about 22% in slopes of BSA and G-CSF calibration curves was observed (Fig. 5). The concentration of G- SCF in a 4 times diluted supernatant calculated from G-CSF and BSA calibration curves was 5.71 µg/ml and 1.11 µg/ml, respectively. Mindful of such a big difference in the calculated concentrations it was decided to use a value of G-CSF concentration calculated form G-CSF calibration curve. The concentration of G-CSF in the solution, which was used for the modification of MagBs, decreased from 50 µg/ml (initial concentration) to 22.8 µg/ml (in supernatant). The results of the Bradford assay showed that during the modification procedure more than a half of G-CSF proteins were immobilized on the surface of MagBs. The amount of immobilized G-CSF in the initial MagBs-G solution was 5.44 µg. MagBs-G concentration in initial solution was 500 µg/ml.

NFS-60 cells were treated with a different concentration of MagBs-G for 48 h. In addition, the investigation of NFS-60 cell proliferation in the presence of free G-CSF was done in parallel. Cell proliferation and

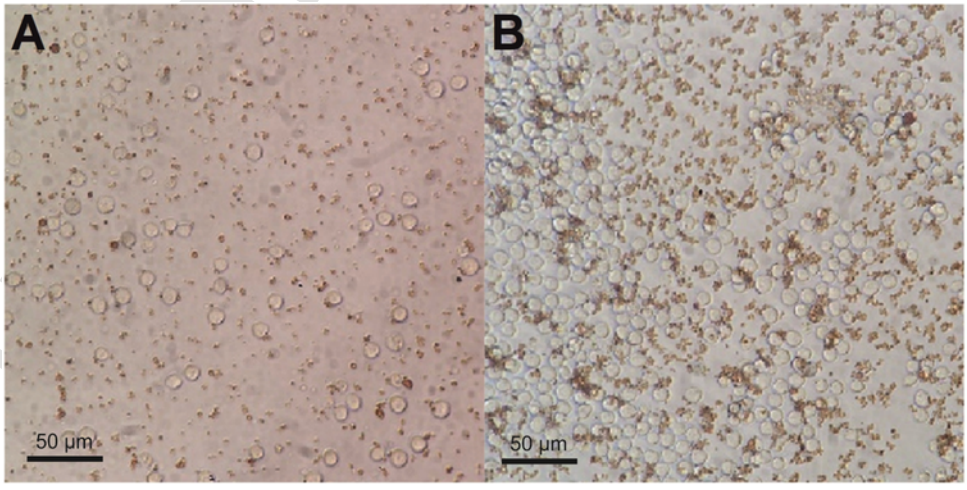

Fig. 3. Optical microscopy images of cells (**A**) immediately after addition of MagBs (c_{MagBs}- 50 µg/ml) and (**B**) after 48 h of cultivation.

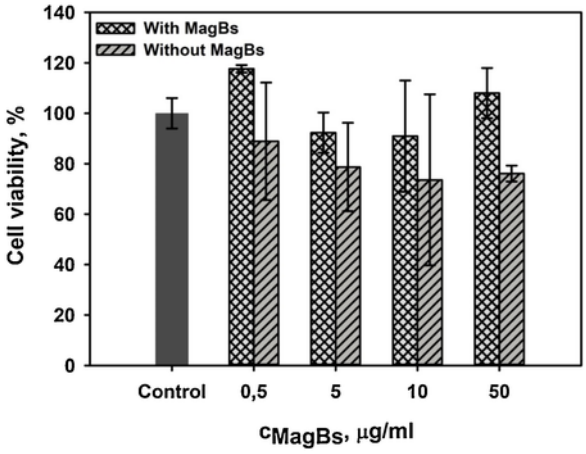

Fig. 4. Dependency of cell viability on MagBs concentration after 48 h of incubation. Control group is NFS-60 cells which were incubated without MagBs.

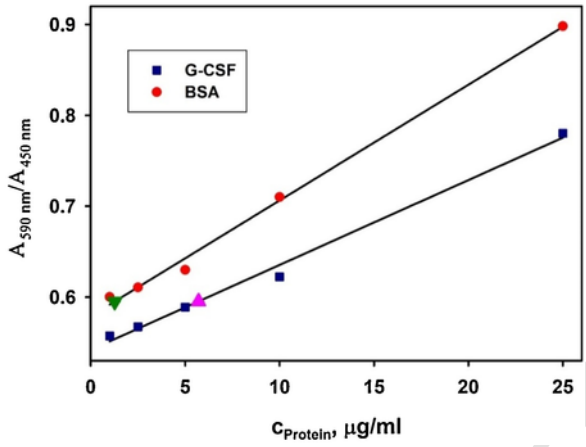

Fig. 5. Calibration curves of BSA (circles) and G-CSF (squares) diluted in PBS. Triangles — points for the evaluation of G-CSF concentration in 4 times diluted supernatant after the MagBs modification procedure using calibration curve of BSA (▼) and using calibration curve of G-CSF (▲).

viability was analysed by the XTT assay (Fig. 6). The concentration of MagBs-G in a 96-well microplate was recalculated to the concentration of G-CSF. The selection of free G-CSF concentrations used for proliferation test was based on the concentration of G-CSF in solutions of MagBs-G. It was decided to use a G-CSF concentration from 0.01 µg/ml to 1 µg/ml. As we expected the proliferation of NFS-60 cells in the used range of free G-CSF was higher in comparison with the control group, however no difference in the response was observed when increasing the concentration of G-CSF in the selected concentrations range (Fig. 6A). Furthermore, MagBs-G concentration effect on NFS-60 cell proliferation was investigated in the range from 0.5 µg/ml to 50 µg/ml of MagBs-G which relates to a G-SCF concentration in the range from 0.027 µg/ml to 2.7 µg/ml. Gradual increase of proliferation when increasing MagBs-G concentration was observed in all test wells (Fig. 6B). The proliferation ability increased almost twofold when 0.5 µg/ml of MagBs-G (0.027 µg/ml of G-CSF) was used, but it was about three times lower than that for the samples with free G-CSF. The maximal proliferation, which was reached using free G-CSF, was achieved only at the highest concentration of MagBs-G (50 µg/ml). The stimulation effect on NFC-60 cell proliferation also was observed by other authors using 50 nm diethylenetriaminepentaacetic acid functionalized SiO_2 particles modified with G-CSF [35]. Thus, G-CSF molecules retained their activity after immobilization. In our case a relatively high concentration of immobilized G-CSF (2.7 µg/ml) required in test wells with NFS-60 cells to achieve maximal proliferative response can be explained by a random orientation of covalently immobilised G-CSF molecules on MagBs surface. Accordingly, not all molecules of G-CSF could improve the proliferation of NFS-60 cells. In addition, the mobility of MagBs-G is limited due to their size, therefore it is more difficult for G-CSF molecules that are immobilized on surface of particles to reach NFS-60 cells compared to free G-CSF molecules and it takes more time. In addition, not all G-CSF molecules immobilized on MagBs surface can approach receptors on cells due to spatial hindrances.

A proliferation response in the previous test (Fig. 6A) was maximal when NFS-60 cells were incubated even with the lowest used free G-CSF concentration (0.01 µg/ml). Therefore, for the evaluation and comparison of the potency of free and immobilized on MagBs surface G-CSF additional test was performed. NFS-60 cells were incubated with various free G-CSF concentrations in the range from 0 to 1 ng/ml. Obtained results are represented in form of dose-response curves (Fig. 7A). In the case of free G-CSF half-maximal response (EC_{50}) value (the concentration of G-CSF that gives half-maximal response) was about 68 pg/ml or 3.6 pM, which is comparable with results of other authors (5.3 pM [42]). The 100% viability was achieved in the presence of 1 ng/ml of free G-CSF in the cell medium. A similar G-CSF concentration (2 ng/ml) was also needed for reaching 100% viability in the previously reported paper [43]. In the case of G-CSF immobilized on MagBs surface (Fig. 7B) an EC_{50} value was 214 ng/ml or 11.4 nM. Such big difference in EC_{50} values between the free and immobilized G-CSF indicated that free G-CSF molecules possess higher potency than on MagBs immobilized G-CSF. Nevertheless, it is possible to achieve the same efficiency of free and immobilized G-CSF molecules on the prolif-

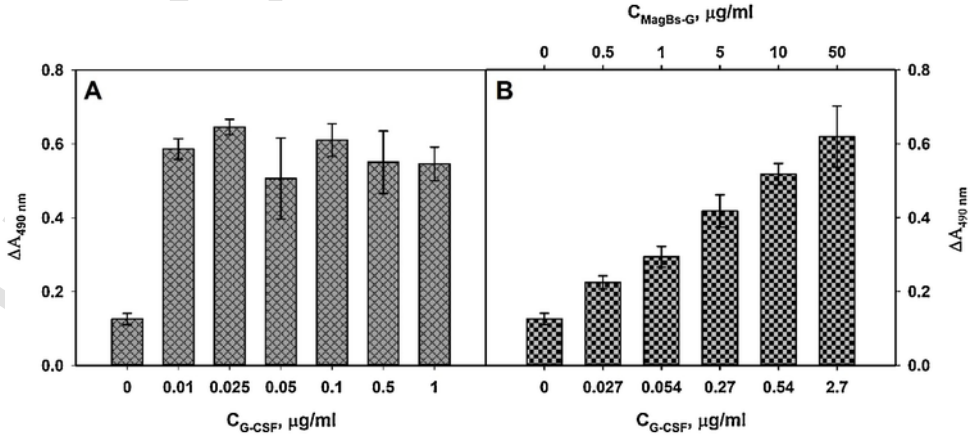

Fig. 6. Comparison of XTT colorimetric measurements of the NFS-60 cell proliferation, incubating cells with a different concentration of (**A**) free G-CSF and (**B**) MagB-G.

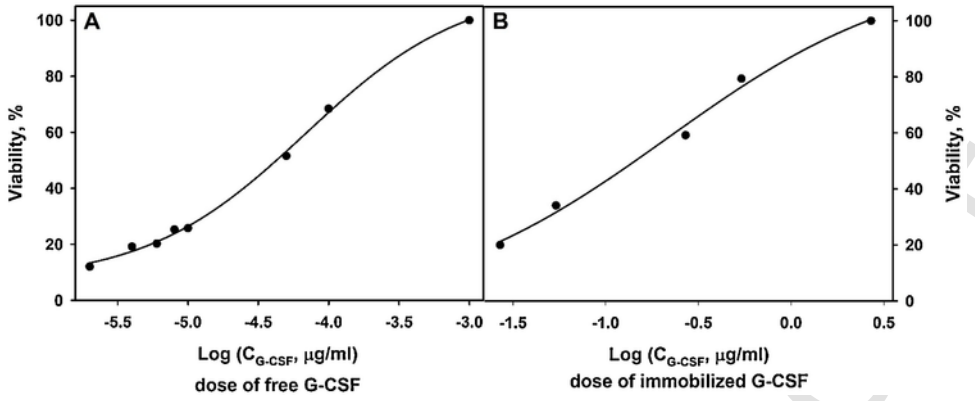

Fig. 7. Dose-response curves of (**A**) free and (**B**) immobilized on MagBs surface G-CSF molecules using NFS-60 cell line.

eration of cells (Fig. 6), however the amount of MagBs-G or the initial amount of G-CSF used for MagBs surface modification must be higher.

The specific activity of G-CSF after immobilization on MagBs surface was tested. G-CSF molecules even after the immobilization on beads affect the proliferation of NFS-60 cells. Sufficiently higher concentration of MagBs-G is required to achieve maximal proliferation response in comparison with free G-CSF molecules, even though in both cases G-CSF molecules possess the same efficacy. EC_{50} value of free G-CSF is quite lower in comparison with EC_{50} value of immobilized G-CSF. Such notable difference in the potency of G-CSF might be explained by non-optimal, random orientation of G-CSF on the surface of MagBs after covalent bonding. Another limiting factor on the proliferation efficiency is the restriction of MagBs-G mobility and spatial hindrances. Additionally, G-CSF and its receptor complex requires 2:2 stoichiometry to be effective [44–46], which means that the distance between immobilized G-CSF molecules and their orientation needs to be taken into consideration. These problems could be solved by using smaller magnetic particles, managing the surface coverage of protein on the particle and by ensuring a proper orientation of molecules. Normally, activation signal after ligand – receptor complex formation is transferred to a signal transducer and activator of transcription (STAT) families' proteins. Then activation signal is transmitted to phosphatidylinositol 3 kinase and its ligand Akt, and finally to the $p21^{ras}$/Raf/MAPK pathway [47]. To understand how immobilized G-CSF activate the cascade of actions, additional experiments are needed taking in to account that G-CSF-mediated signal transduction is accompanied by receptor mediated endocytosis [47].

4. Conclusions

In this work silica coated magnetic particles with free carboxyl groups were chosen as matrix for the easy protein immobilization and separation. It was shown that MagBs were not cytotoxic for NFS-60 cells and their presence in a cell medium has no influence on the cell viability. Silica matrix is likely the reason of reduced Fe_3O_4 cytotoxic effect. The immobilization of G-CSF molecules on MagBs surface was successfully performed. The usage of magnetic particles allows to accelerate the process of covalent immobilization of G-CSF and to avoid the centrifugation step, which is usually required for the collection of modified particles during various steps of modification. Therefore, in such way the loss of G-CSF-modified particles is significantly reduced and outcome of modification is increased, which is especially important when a protein such as G-CSF with a relatively high production cost is used for the development of new drugs.

Acknowledgments

This work is part of a project that has received funding from the European Union's Horizon 2020 research and innovation programme under grant agreement No 778157 CanBioSe. The authors want to thank Lina Jonuskaite for her contribution in experiments.

References

[1] T. Jamshaid, E.T.T. Neto, M.M. Eissa, N. Zine, M.H. Kunita, A.E. El-Salhi, A. Elaissari, Magnetic particles: from preparation to lab-on-a-chip, biosensors, microsystems and microfluidics applications, Trac Trends Anal. Chem. 79 (2016) 344–362.
[2] L. Moro, M. Turemis, B. Marini, R. Ippodrino, M.T. Giardi, Better together: strategies based on magnetic particles and quantum dots for improved biosensing, Biotechnol. Adv. 35 (2017) 51–63.
[3] B.-H. Lai, C.-C. Yeh, D.-H. Chen, Surface modification of iron oxide nanoparticles with polyarginine as a highly positively charged magnetic nano-adsorbent for fast and effective recovery of acid proteins, Process Biochem. 47 (2012) 799–805.
[4] Z. Ma, H. Liu, Synthesis and surface modification of magnetic particles for application in biotechnology and biomedicine, China Particuol. 5 (2007) 1–10.
[5] I.K. Puri, R. Ganguly, Particle transport in therapeutic magnetic fields, Annu. Rev. Fluid Mech. 46 (2014) 407–440.
[6] X. Pan, G. Zuo, T. Su, S. Cheng, Y. Gu, X. Qi, W. Dong, Polycarboxylic magnetic polydopamine sub-microspheres for effective adsorption of malachite green, Colloids Surf. A Physicochem. Eng. Aspects 560 (2019) 106–113.
[7] Z. Sun, X. Zhou, W. Luo, Q. Yue, Y. Zhang, X. Cheng, W. Li, B. Kong, Y. Deng, D. Zhao, Interfacial engineering of magnetic particles with porous shells: towards magnetic core – porous shell microparticles, Nano Today 11 (2016) 464–482.
[8] F. Rusmini, Z. Zhong, J. Feijen, Protein immobilization strategies for protein biochips, Biomacromolecules 8 (2007) 1775–1789.
[9] F. Rehm, S. Chen, B. Rehm, Enzyme engineering for in situ immobilization, Molecules 21 (2016) 1370.
[10] P. Azcona, I. López-Corral, V. Lassalle, Fabrication of folic acid magnetic nanotheranostics: an insight on the formation mechanism, physicochemical properties and stability in simulated physiological media, Colloids Surf. A Physicochem. Eng. Aspects 537 (2018) 185–196.
[11] N.V. Mdlovu, F.A. Mavuso, K.-S. Lin, T.-W. Chang, Y. Chen, S.S.S. Wang, C.-M. Wu, N.B. Mdlovu, Y.-S. Lin, Iron oxide-pluronic F127 polymer nanocomposites as carriers for a doxorubicin drug delivery system, Colloids Surf. A Physicochem. Eng. Aspects 562 (2019) 361–369.
[12] S. Berensmeier, Magnetic particles for the separation and purification of nucleic acids, Appl. Microbiol. Biotechnol. 73 (2006) 495–504.
[13] I.M. Hsing, Y. Xu, W. Zhao, Micro-and nano-magnetic particles for applications in biosensing, Electroanalysis 19 (2007) 755–768.
[14] A. Hecht, P. Commiskey, N. Shah, R. Kopelman, Bead assembly magnetorotation as a signal transduction method for protein detection, Biosens. Bioelectron. 48 (2013) 26–32.
[15] K.W. Bong, S.C. Chapin, P.S. Doyle, Magnetic barcoded hydrogel microparticles for multiplexed detection, Langmuir 26 (2010) 8008–8014.
[16] N. Panagiotopoulos, R.L. Duschka, M. Ahlborg, G. Bringout, C. Debbeler, M. Graeser, C. Kaethner, K. Lüdtke-Buzug, H. Medimagh, J. Stelzner, T.M. Buzug, J. Barkhausen, F.M. Vogt, J. Haegele, Magnetic particle imaging: current developments and future directions, Int. J. Nanomed. 10 (2015) 3097–3114.
[17] I.L. Sokolov, V.R. Cherkasov, A.V. Vasilyeva, V.A. Bragina, M.P. Nikitin, Paramagnetic colloidal ferrihydrite nanoparticles for MRI contrasting, Colloids Surf. A Physicochem. Eng. Aspects 539 (2018) 46–52.
[18] M. Mahmoudi, K. Azadmanesh, M.A. Shokrgozar, W.S. Journeay, S. Laurent, Effect of nanoparticles on the cell life cycle, Chem. Rev. 111 (2011) 3407–3432.

[19] E. Roeder, C. Henrionnet, J.C. Goebel, N. Gambier, O. Beuf, D. Grenier, B. Chen, P.-A. Vuissoz, P. Gillet, A. Pinzano, Dose-response of superparamagnetic iron oxide labeling on mesenchymal stem cells chondrogenic differentiation: a multi-scale in vitro study, PLoS One 9 (2014), e98451.
[20] B.D. Plouffe, S.K. Murthy, L.H. Lewis, Fundamentals and application of magnetic particles in cell isolation and enrichment: a review, Rep. Prog. Phys. 78 (2014), 016601.
[21] Y.-T. Chen, A.G. Kolhatkar, O. Zenasni, S. Xu, T.R. Lee, Biosensing using magnetic particle detection techniques, Sensors 17 (2017) 2300.
[22] J. Hoggatt, L.M. Pelus, New G-CSF agonists for neutropenia therapy, Expert Opin. Investig. Drugs 23 (2014) 21–35.
[23] B. Huggett, J. Hodgson, R. Lähteenmäki, Public biotech 2010—the numbers, Nat. Biotechnol. 29 (2011) 585.
[24] M. Foote, G. Morstyn, Granulocyte Colony-Stimulating Factor: Biology and Clinical Potential, Principles of Cancer biotherapy, Springer, 2009569–580.
[25] M. Foote, G. Morstyn, Granulocyte-macrophage colony-stimulating factor, in: R.K. Oldham, R.O. Dillman (Eds.), Principles of Cancer Biotherapy, Springer Netherlands, Dordrecht, 2009, pp. 581–588.
[26] A. Oishi, A. Otani, M. Sasahara, H. Kojima, H. Nakamura, Y. Yodoi, N. Yoshimura, Granulocyte colony-stimulating factor protects retinal photoreceptor cells against light-induced damage, Invest. Ophthalmol. Vis. Sci. 49 (2008) 5629–5635.
[27] J. Wang, L. Yao, S. Zhao, X. Zhang, J. Yin, Y. Zhang, X. Chen, M. Gao, E.-A. Ling, A. Hao, Granulocyte-colony stimulating factor promotes proliferation, migration and invasion in glioma cells, Cancer Biol. Ther. 13 (2012) 389–400.
[28] M. Hara, S. Yuasa, K. Shimoji, T. Onizuka, N. Hayashiji, Y. Ohno, T. Arai, F. Hattori, R. Kaneda, K. Kimura, G-CSF influences mouse skeletal muscle development and regeneration by stimulating myoblast proliferation, J. Exp. Med. (2011), 20101059, jem.
[29] G. Mickiene, I. Dalgediene, Z. Dapkunas, G. Zvirblis, H. Pesliakas, A. Kaupinis, M. Valius, E. Mistiniene, M. Pleckaityte, Construction, purification, and characterization of a homodimeric granulocyte colony-stimulating factor, Mol. Biotechnol. 59 (2017) 374–384.
[30] Y. Weinstein, J.N. Ihle, S. Lavu, E.P. Reddy, Truncation of the c-myb gene by a retroviral integration in an interleukin 3-dependent myeloid leukemia cell line, Proc. Natl. Acad. Sci. U. S. A. 83 (1986) 5010–5014.
[31] S. Matsuda, N. Shirafuji, S. Asano, Human granulocyte colony-stimulating factor specifically binds to murine myeloblastic NFS-60 cells and activates their guanosine triphosphate binding proteins/adenylate cyclase system, Blood 74 (1989) 2343–2348.
[32] D.A. Scudiero, R.H. Shoemaker, K.D. Paull, A. Monks, S. Tierney, T.H. Nofziger, M.J. Currens, D. Seniff, M.R. Boyd, Evaluation of a soluble tetrazolium/formazan assay for cell growth and drug sensitivity in culture using human and other tumor cell lines, Cancer Res. 48 (1988) 4827–4833.
[33] S.C. McBain, H.H.P. Yiu, J. Dobson, Magnetic nanoparticles for gene and drug delivery, Int. J. Nanomed. 3 (2008) 169–180.
[34] G. De Crozals, D. Kryza, G.J. Sánchez, S. Roux, D. Mathé, J. Taleb, C. Dumontet, M. Janier, C. Chaix, Granulocyte colony-stimulating factor nanocarriers for stimulation of the immune system (Part I): synthesis and biodistribution studies, Bioconjug. Chem. 29 (2017) 795–803.
[35] D. Kryza, G. De Crozals, D. Mathe, J. Taleb Sidi-Boumedine, M. Janier, C. Chaix, C. Dumontet, Granulocyte-colony stimulating factor nanocarriers for stimulation of the immune system (Part II): dose-dependent biodistribution and in vivo antitumor efficacy in combination with rituximab, Bioconjug. Chem. 29 (2017) 804–812.
[36] J. Zaloga, C. Janko, R. Agarwal, J. Nowak, R. Müller, A.R. Boccaccini, G. Lee, S. Odenbach, S. Lyer, C. Alexiou, Different storage conditions influence biocompatibility and physicochemical properties of iron oxide nanoparticles, Int. J. Mol. Sci. 16 (2015) 9368–9384.
[37] E.L. Brito, D.N. Gomes, C.C. PláCid, J.C.R. de Araújo, F. Bohn, L. Streck, J.L.C. Fonseca, Superparamagnetic magnetite/IPEC particles, Colloids Surf. A Physicochem. Eng. Aspects 560 (2019) 376–383.
[38] M.V. Berridge, P.M. Herst, A.S. Tan, Tetrazolium dyes as tools in cell biology: new insights into their cellular reduction, Biotechnol. Annu. Rev. 11 (2005) 127–152.
[39] T. Marshall, K.M. Williams, Bradford protein assay and the transition from an insoluble to a soluble dye complex: effects of sodium dodecly sulphate and other additives, J. Biochem. Biophys. Methods 26 (1993) 237–240.
[40] S.C. Silvério, S. Moreira, A.M.F. Milagres, E.A. Macedo, J.A. Teixeira, S.I. Mussatto, Interference of some aqueous two-phase system phase-forming components in protein determination by the Bradford method, Anal. Biochem. 421 (2012) 719–724.
[41] P. Nicolás, V.L. Lassalle, M.L. Ferreira, Quantification of immobilized Candida antarctica lipase B (CALB) using ICP-AES combined with Bradford method, Enzyme Microb. Technol. 97 (2017) 97–103.
[42] Y. Bai, D.K. Ann, W.-C. Shen, Recombinant granulocyte colony-stimulating factor-transferrin fusion protein as an oral myelopoietic agent, Proc. Natl. Acad. Sci. 102 (2005) 7292–7296.
[43] N. Conzelmann, A. Schneider, A screen for peptide agonists of the G-CSF receptor, BMC Res. Notes 4 (2011) 194.
[44] J.E. Layton, N.E. Hall, The interaction of G-CSF with its receptor, Front. Biosci. 11 (2006) 3181–3189.
[45] M. Aritomi, N. Kunishima, T. Okamoto, R. Kuroki, Y. Ota, K. Morikawa, Atomic structure of the GCSF–receptor complex showing a new cytokine–receptor recognition scheme, Nature 401 (1999) 713.
[46] T. Tamada, E. Honjo, Y. Maeda, T. Okamoto, M. Ishibashi, M. Tokunaga, R. Kuroki, Homodimeric cross-over structure of the human granulocyte colony-stimulating factor (GCSF) receptor signaling complex, Proc. Natl. Acad. Sci. 103 (2006) 3135–3140.
[47] L.H. Aarts, O. Roovers, A.C. Ward, I.P. Touw, Receptor activation and 2 distinct COOH-terminal motifs control G-CSF receptor distribution and internalization kinetics, Blood 103 (2004) 571–579.